# Photosensitive acrylates containing bio-based epoxy-acrylate soybean oil for 3D printing application

# PHOTOSENSITIVE ACRYLATES CONTAINING BIO-BASED EPOXY-ACRYLATE SOYBEAN OIL FOR 3D PRINTING APPLICATION

Giuseppe Rosace[1], Raphael Palucci Rosa[2,*], Rossella Arrigo[3], Giulio Malucelli[3]

[1] Department of Engineering and Applied Sciences, University of Bergamo, and Local INSTM Unit, Viale Marconi 5, 24044, Dalmine, BG, Italy.

[2] Department of Engineering and Applied Sciences, University of Bergamo, Viale Marconi 5, 24044, Dalmine, BG, Italy.

[3] Department of Applied Science and Technology, Politecnico di Torino, and Local INSTM Unit, Viale T. Michel 5, 15121, Alessandria, Italy.

*E-mail address: raphael.rosa@unibg.it

**ABSTRACT**

Stereolithography (SLA) is a 3D-printing process that is rapidly shifting from being an expensive and limited technology to an affordable, precise, and fast method of mass production. However, most of the current resins are petroleum-based, which makes them toxic, non-degradable and with poor biocompatibility. In this study, a standard petroleum-based resin containing urethane acrylate and acrylic monomers was combined with epoxy-acrylate soybean oil (EASO), aiming to reduce its impact on the environment. Ratios varying from 10 to 50 wt.% of EASO were incorporated into the commercial resin while maintaining the viscosity low, between 0.27 and 1.06 Pa s. The printed samples showed good quality and complete integration between the layers. The addition of 50 wt.% of EASO increased the samples elongation at break by 108% (from 2.3% to 4.8%) and decreased the contact angle by 26.4% (from 72º to 53º).

Moreover, the mixture showed good thermal and swelling stability and tensile strength in the range of other commercial cured systems. The addition of EASO may significantly contribute to the exploitation of greener materials, which well matches today's circular economy concept.

## 1 INTRODUCTION

Additive manufacture (AM), also known as 3D printing, is revolutionizing the entire industrial sector, from the production of simple, daily disposable products to high precision medical devices and aerospace components.[1,2] 3D printing has many advantages over traditional manufacturing techniques, including generating less waste, freedom of design, market adaptability and the production of complex structures.[3,4] Moreover, it is possible to fabricate structures from a variety of materials, such as metals, ceramics, woods, thermosets and photosensitive polymer liquids.[5]

Stereolithography (SL), one of the earliest AM technologies,[3] uses photosensitive polymers resins and a light source (emission wavelength between 350 and 405 nm) to print high detailed parts in a layer-by-layer process and is able to achieve resolutions down to 5 microns.[11] It accounts for nearly half of the AM market nowadays,[12] and it is proving to be an economical method to produce highly accurate parts having good thermal, mechanical and chemical properties.[13]

The photosensitive resins used on stereolithography printers are usually made of a combination of photosensitive liquid acrylates and epoxy monomers/oligomers with a suitable photoinitiator.[16] The polymerization reaction of acrylate differs from that of epoxy-based resins.[10] Acrylate-based resins undergo free radical polymerization, which is highly reactive with fast curing time. However, the final parts have low mechanical properties due to the disordered growth of crosslinks. On the other hand, epoxy resins have a more organized chain growth since ~~the~~ they undergo a step-grow polymerization reaction. This leads to final products with better mechanical properties, but requires longer curing times.[16] Additives –as optical

absorbers, stabilizers, fillers can also be incorporated into the resin to improve its mechanical properties, to decrease the reaction time or to provide new functionalities.[10]

Most available resins nowadays are derived from petroleum, which raises many environmental concerns, such as $CO_2$ emission, plastic waste and materials toxicity.[17] According to Lebreton et al.[18] projections, if humanity maintains the current rate of plastic waste production, it will generate 380 million metric tons (Mt) in 2060, a 90% increase from what was produced in 2020 (200 Mt).[18] Part of the plastic waste will come from AM, since the 3D printing market is expected to continue to monotonically grow, with the industries transiting to it.[12] Thus, the development of biobased resins has become essential to reduce the environmental impact of the currently employed resins.

To address the lack of biobased photocurable resins, few studies started to design new resin formulations. Dijkstra et al.[16] proposed a biodegradable resin for multiple applications using biodegradable acrylate monomers and oligomers. The designed resin systems showed similar mechanical properties with respect to standard non-renewable resins. Palaganas-et al.[19] developed a biocompatible resin for medical applications by combining poly(ethylene)diacrylate (PEGDA) with cellulose nanocrystals (CNCs). More recently, Bassett et al.[20] prepared a biobased resin by reacting vanillin with methacrylic anhydride. Their results demonstrated that the samples had good mechanical properties and high Tg, showing some potential to substitute petroleum-based resins.

Another promising way for creating biobased systems is the usage of plant oils, particularly interesting are soybean oil, linseed oil and castor oil.[21–23] They are available worldwide, have relatively low production costs and are already used to produce UV-curable coatings, monomers, oligomers and bio-composites.[23–25] Principally, soybean oil since it is the most globally produced oil nowadays and has already been modified for formulating UV-curable resins.[17,21,26–28] Guit et al.[21] utilized epoxidized soybean oil (ESO) and di- and

trifunctional epoxidized soybean oil methacrylate ($ESOMA_2$ and $ESOMA_3$, respectively) with biobased diluents and bio-(meth)acrylate oligomers to formulate a SL resin. The SL resins had bio-renewable carbon content between 77 to 80%, viscosities of 0.5 to 1.5 Pa·s and showed tensile strength and elongation at break similar to fossil-based counterparts.[21] Cui et al.[17] added urethane-modified soybean oil with an epoxy group (SBO-URE) into a acrylate-based resin to set a dual-curing hybrid system. The addition of SBO-URE showed an overall improvement of the mechanical strength of the parts without affecting their elongation.[17]

Epoxy-acrylate soybean oil (EASO), another derivative from soybean oil, was used to develop SL resins as well. EASO is a high viscous liquid and contains a high concentration of various functional groups such as acrylic, epoxy, and hydroxy groups.[28,29] EASO has been successfully used for the development of 4D scaffolds;[23] more recently, Lebedevaite et al.[30] combined EASO with commercially available bio-based materials to develop a resin for printing complex structures. Their resins showed a biorenewable carbon content within 75 and 82%, a high curing rate and tunable mechanical properties. However, there is still a limited number of studies about the usage of EASO for 3D printing.

In this study, we preliminary investigate the effect of the presence of different EASO loadings on the final properties (namely, thermal, mechanical, and structural) of a commercially available SLA formulation. The reduction in fossil-derived compounds and the simple procedure developed (not requiring complicated purification steps) suggest the proposed protocol as a promising solution for industrial-scale exploitation, reducing the environmental impact and fulfilling the circular economy concept.

## 2 EXPERIMENTAL

### 2.1 Materials

Epoxy-acrylate soybean oil (EASO, containing 4,000 ppm monomethyl ether hydroquinone as inhibitor), and Diphenyl(2,4,6-trimethylbenzoyl) phosphine oxide (TPO) were purchased from Merck KGaA (Darmstadt, Germany). Isopropanol (≥ 99%) was received from Carlo Erba. Peopoly Moai standard clear resin (PY) was purchased from 3Dpartnershop company: it is an acrylic-based photopolymer designed for the Moai printer, containing urethane acrylate (30-50%), bisphenol A ethoxylate diacrylate (30-50%) and benzophenone as the photoinitiator (5 wt.%). All products were used as received.

### 2.2 Photocurable resin formulation

The photocurable formulations for 3D printing were prepared by mixing different weight ratios of epoxy-acrylate soybean oil (namely 10, 20, 30, 40 and 50 wt.%) with Peopoly Moai standard resin without the addition of photoinitiator, as it is already present in the formulation of the commercial resin. However, by increasing the amount of soybean oil, the photoinitiator already added to the PY resin may not be enough to drive the polymer network formation. To investigate the influence of the photoinitiator on the photocuring process of the formulation with the highest concentration of soybean oil (i.e. 50 wt.%), 1 wt.% of TPO was added. This formulation was then ultrasonicated for 60 min at 30 ºC to thoroughly dissolve the photoinitiator. The resulting solutions were vigorously stirred for 30 min at 40 ºC, and then, allowed to rest in the dark until bubbles were no longer present. Each composition was prepared in a room with minimal ambient light and stored in a dark place.

## 2.3 3D printing of samples

A Peopoly Moai 130 SLA 3D-printer with an easy-to-level build plate was used to print samples suitable for the different testing. The machine was equipped with a solid-state laser with frequency conversion emitting at 405 nm with a power of 150 mW. It was set to operate at standard configurations when printing with commercial resins. The 3D models were created using FreeCad software, and the printing layer height was set at 0.1 mm. The laser power and initial exposure time were adjusted when printing the biobased resins. In this case, the power level was set to 58 mW and initial exposure time raised from 40 to 60 seconds. All samples were printed at 30 ºC using a built-in heater to maintain the temperature constant. These parameters were tuned to improve the quality of the printing and do not affect the samples mechanical properties. Before transferring the reinforced resin into the vat, the mixture was slowly stirred for 30 min at 40 ºC. After printing, all samples were carefully removed from the build platform. To eliminate any unreacted monomer, they were washed alternatively 3 times, each with isopropanol and water, before drying them in the dark for one day. Finally, all printed samples were placed in a UV chamber, using a 405 nm mercury lamp (60 W, Peopoly) for the post-curing step under UV irradiation for 60 min to ensure the completeness of the curing process.

## 2.4 FT-IR Spectroscopy

ATR-FTIR spectroscopy was used to confirm the occurrence of the polymerization process under UV irradiation by observation of the signals of key functional groups. The infrared analysis was performed using a Thermo Avatar 370 spectrophotometer equipped with an attenuated total reflectance (ATR) device with diamond crystal for solids analysis. Using Omnic 7.3 software, the spectra were collected in absorbance mode with a resolution of 4 $cm^{-1}$ and 32 scans per measurement, within 2000 and 650 $cm^{-1}$, using 3D printed dog-bone

specimens. Additionally, as the amount of photoinitiator in the Peopoly resin formulation might not be enough for curing the mixtures containing increasing EASO loadings, a 3D-printed sample containing 50:50 EASO-Peopoly mixture with 1 wt.% of TPO as photoinitiator was produced and tested.

### 2.5 Rheological analyses

Rheological measurements were performed using an ARES (TA Instrument) strain-controlled rheometer in parallel plate geometry (plate diameter: 50 mm; gap between the plates: 0.7 mm). The complex viscosity of the samples was measured at 25 °C through strain sweep measurements in a range of strain amplitude from 1 to 400%. In all the tests, the frequency was fixed at 1 rad $s^{-1}$.

### 2.6 Tensile tests

All tensile tests were performed in accordance with ASTM D638. For each PY/EASO ratio five test parts were printed with a dog-bone shape with the dimension of 63.5×9.53×3.2 mm (L×W×H) and with 3.2 mm width in the narrow section. All samples were post-cured for 60 min under UV radiation prior to testing. The samples were tested on a Galdabini Sun 5 at room temperature with a 30 N load cell and using a crosshead speed of 1 mm $min^{-1}$. Tensile strength (MPa) and elongation at break (%) were determined using the average of the five tests; Young's modulus (MPa) and fracture energy (mJ) were evaluated as well.

### 2.7 Thermogravimetric analysis

The thermal and thermo-oxidative stability of the post-cured products containing EASO was evaluated by means of thermogravimetric analyses (TGA). The analysis was carried out on a Discovery apparatus (TA Instruments), using a heating rate of 10 °C $min^{-1}$, under both

nitrogen and airflow (35 and 25 ml $min^{-1}$, respectively). The experimental error was ± 0.5% on the weight and ± 1 °C on the temperature.

### 2.8 Contact angle measurement

Static contact angle values of PY, EASO and PY/EASO mixtures were measured by a homemade instrument equipped with a high-speed CCD camera. The used equipment allows the determination of contact angle, with a precision of ± 1°, by taking images at frequencies as high as 200 Hz, starting within a few tens of milliseconds after the deposition of the drop. All measurements were performed under ambient atmosphere at room temperature and 40 ± 5% relative humidity. Five rectangular shape parts with 50×25×1 mm was 3D printed for each sample. A small drop of high purity distilled water was placed on the surface of the samples, and the image of the droplet was recorded after 10s. The drop volume was taken within the range where the contact angle did not change with the variation of the volume (i.e. 4 ± 0.5 µl). The contact angle (CA) values were determined using image analysis software. The reproducibility of the angle was within ± 1.5°.

### 2.9 Swelling ratio

Rectangular samples (30×10×5 $mm^3$) were printed with different PY/EASO weight ratios and post-cured for 60 min. The samples were weighted ($M_1$) and then dipped in deionized water for 30 days. Every 5 days, the samples were taken from the liquid, removing the water excess with towel paper, and then weighted again ($M_2$). At least five specimens were analyzed for each EASO loading. The swelling ratio, $S_w$, was calculated using Equation 1 below:

$$S_w = \frac{(M_2 - M_1)}{M_1} \times 100 \qquad \text{Equation 1}$$

### 2.10 Statistical analysis

Statistical analysis was done with one-way analysis of variance (ANOVA), with the level of significance set at $p < 0.05$, using R software (R Fundation corp). The results are presented as means ± standard deviations (S.D.) of at least five independent sets of measurements.

## 3 RESULTS AND DISCUSSION

### 3.1 FT-IR analysis

The addition of EASO in the $PY_{uncured}$ dilutes the benzophenone (photoinitiator) present in the commercial resin and could affect its efficacy to drive the UV-curing. To check whether the concentration of benzophenone was enough to perform the UV-curing process, FTIR analysis was carried out on the formulation with the highest concentration of EASO (i.e. $PY_{EASO50}$), either in the presence (sample $EASO_{TPO}$) or without 1 wt.% of TPO, used as an extra photoinitiator (Figure 1a). The photopolymerization reaction was evaluated by monitoring the decrease of double bond peaks at 810 $cm^{-1}$. Indeed, after UV irradiation, the decrease in the peak area at around 810 $cm^{-1}$, assigned to $CH_2$=CH- twisting, indicated that C=C bonds in the reactive monomers took part in the cross-linking reaction. However, since a certain intensity of the band at 810 $cm^{-1}$ was still visible after UV irradiation, three experiments were carried out to investigate the C=C conversion by extending the UV exposure time to 2h ($PY_{cured+2h}$), applying a post-heat treatment ($PY_{thermal}$) and adding a further 5 wt.% photoinitiator ($PY_{TPO5\%}$). In all cases, as shown in Figure 1a, the absorption band at 810 $cm^{-1}$ shows no significant difference. Therefore, the still visible infrared band was assigned to the coating's structure absorption, partially overlapped by C=C vibrations.[31] This finding supports the hypothesis that the benzophenone in the fixed amount was enough to perform the UV-curing of 3D-printed specimens.

After having confirmed that the photoinitiator present in the PY resin was enough to perform the UV-curing reaction, infrared spectra of 3D-printed specimens with increasing concentrations of EASO were acquired. The spectrum of uncured PY resin ($PY_{uncured}$) reveals the presence of C–NH stretching in the urethane unit at 1528 $cm^{-1}$, while the urethane carbonyl and N-H stretching vibrations appear at around 1700 and 3300–3400 $cm^{-1}$, respectively.[32] In particular, the presence of two different absorbance bands at 1720 and 1694.3 $cm^{-1}$, assigned to C=O, is consistent with a different chemical environment for carbonyl groups on monomers. The absorption bands in the range 2860–2950 $cm^{-1}$ are associated with the C-H stretching vibration, while peaks at 1646.9 $cm^{-1}$ and 1615.2 $cm^{-1}$ are assigned to C=C stretching of allylic bond and double-bond present in the alkyl chain, respectively.[33] Both absorption bands at 1235 and 1115 $cm^{-1}$ are ascribed to the -C-O-C- stretching vibration.[34] Finally, an absorption peak can be observed at 810 $cm^{-1}$, indicating the existence of double bonds of the acrylate groups.[35] During the curing process, under UV irradiation, the photoinitiator produces active radicals, opens the double bond groups in the PY monomers, and generates crosslinking, which permits the 3D print specimens to cure. The occurrence of photopolymerization was verified by monitoring the double bond peaks at 1646, 1615 and 810 $cm^{-1}$ through FTIR spectra.[36] At the end of the UV curing step, the peaks of the double bonds are strongly reduced. Furthermore, a small peak change from 1186.1 to 1159.9 $cm^{-1}$ corresponding to the shift of C-O-C groups, provoked by the C=C consumption, is observed. Thus, the reduction of both vinyl functionality of the acrylate polymer absorbance assigned at 985 $cm^{-1}$ and the decrease of the signals at 1410 $cm^{-1}$, related to the consumption of unsaturated double bonds ($CH_2$=CH-R) are observed.[31,37] Accordingly, the peak at around 982 $cm^{-1}$, assigned to the out-of-plane bending vibration and stretching vibration of unsaturated hydrocarbon, also decreased significantly. New absorption bands at around 3369 and 1635 $cm^{-1}$ were assigned to new amide groups obtained by the UV-induced reaction between urethane acrylate and acrylic monomers. Furthermore, all the FTIR

spectra registered from the 3D printed systems containing EASO confirmed the occurrence of the UV-induced polymerization observed for the pure resin ($PY_{uncured}$). The absorption attributed to the stretching of the C=C group is strongly reduced in intensity, suggesting the effective formation of a network of saturated C–C bonds at the expense of soybean oil, urethane acrylic and acrylate groups. As the amount of EASO increases, the absorption bands characteristic of PY decrease their intensity so that, beyond 10 wt.%, the region of the fingerprint changes deeply.

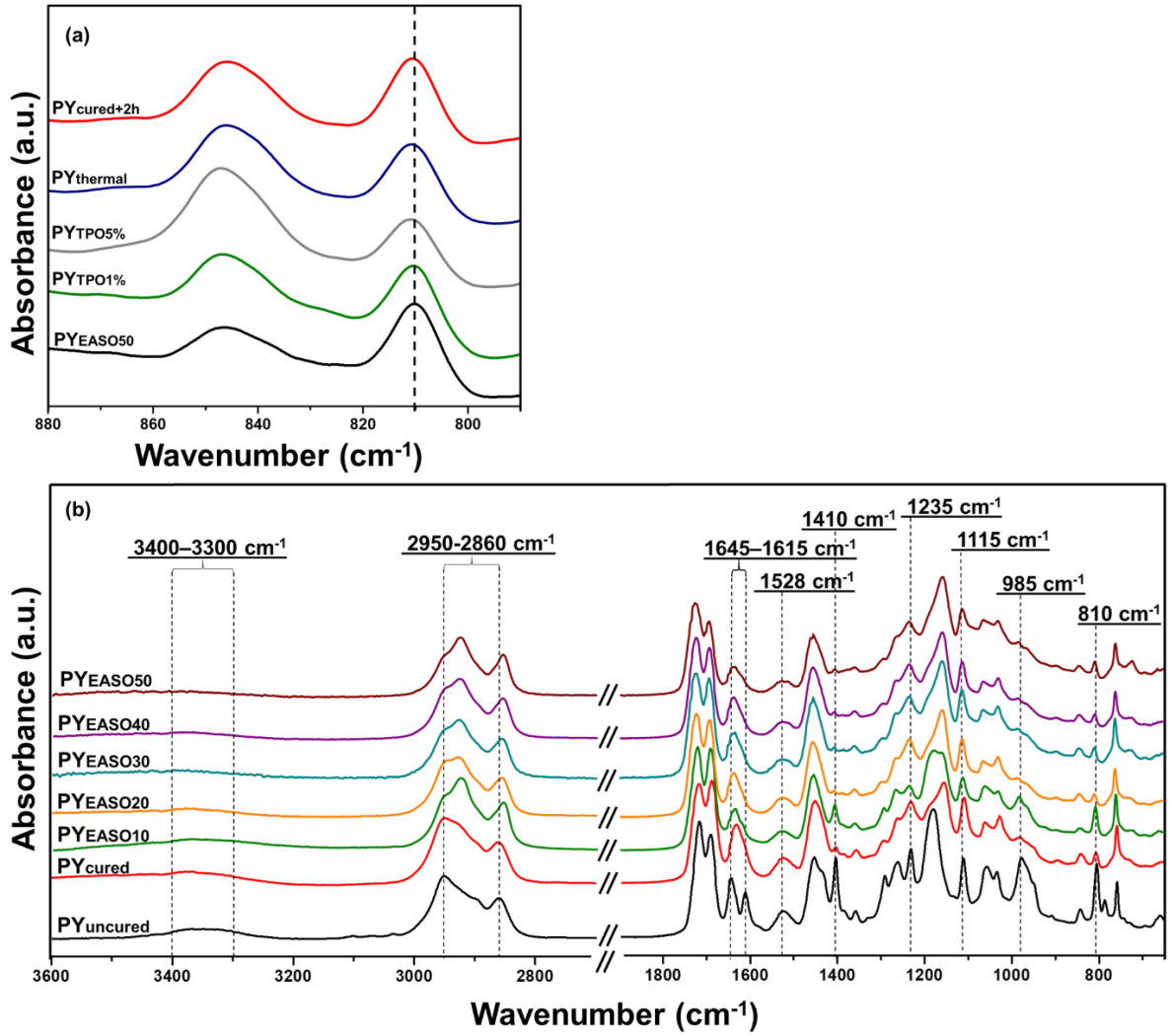

**Figure 1:** (a) FT-IR analysis of $PY_{EASO50}$ with and without TPO and $PY_{EASO}$ submitted to different types of post treatment process in the range of 840 – 800 $cm^{-1}$. (b) Infrared spectra of PY resin with different EASO loadings (varying from 10 to 50 wt.%).

### 3.2 Rheology

The viscosity is a crucial factor that must be taken into consideration when developing a resin for a 3D-printing application. The resin has a few seconds to fill the gap formed between the model and the VAT each time a new layer printed.[38] The viscosity of such commercial resins as Formlabs or Anycubic, is usually between 0.1 and 1.5 Pa s,[20] where the Peopoly moai clear resin exhibits a viscosity of 0.18 Pa s. As reported in Figure 2, EASO shows a viscosity of approximately 15 Pa s at 30 °C, which is too high for most SLA printers. When EASO was combined with the Peopoly resin, the viscosity of the mixtures increased according to the EASO content, from 0.27 to 1.06 Pa s for the formulations containing 10 and 50 wt.% of EASO, respectively. Nevertheless, the introduction of increased EASO loadings did not affect the range of linear viscoelastic behavior of the mixtures and all the samples meet the viscosity requirements for stereolithography applications.

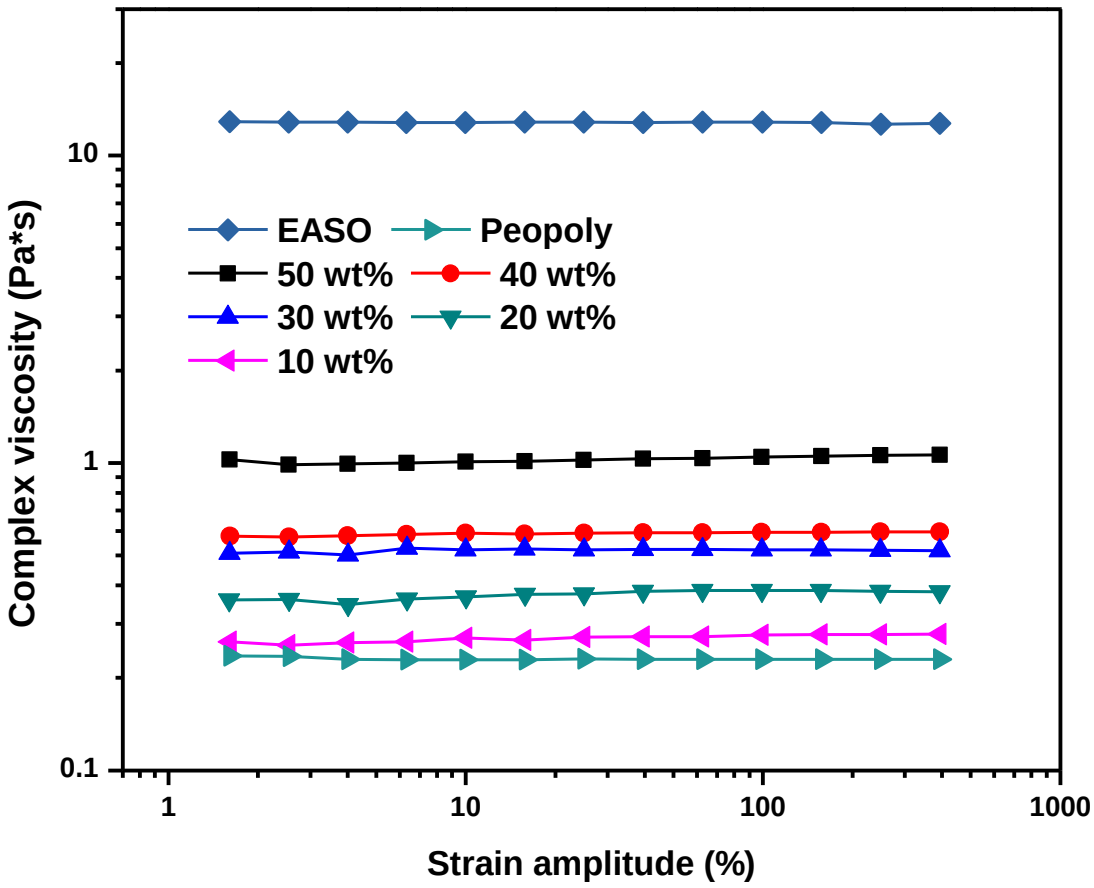


**Figure 2:** Change of PY resin viscosity with different EASO loadings (viscosity curves of neat PY and EASO are also included).

### 3.3 Mechanical properties

A good mechanical behavior is essential for a bio-resin to compete with standard petroleum-based commercial resins.[16] The molecular characteristics of the biomaterial have a strong influence on its mechanical behavior.[21,39] According to Figure 3, the average tensile strength of commercial resins is around 44 MPa (unlike the Peopoly resin standard, for which the average tensile strength is about 50.3 MPa). Our results showed that the presence of 10 wt.% of EASO decreased the tensile strength by approximately 50%, achieving 25 MPa (Figure 4). The tensile strength continued to drop with increasing the EASO content in the mixture, resulting in a 70.8% decrease at the highest EASO loading. The decrease in the tensile strength can be attributed to the network loosening of plant-based resins.[17,40] Nevertheless, the PY

systems containing 10, 20 and 30 wt.% of EASO showed mechanical performances similar to petroleum-based resins (like Anycubic Standard).

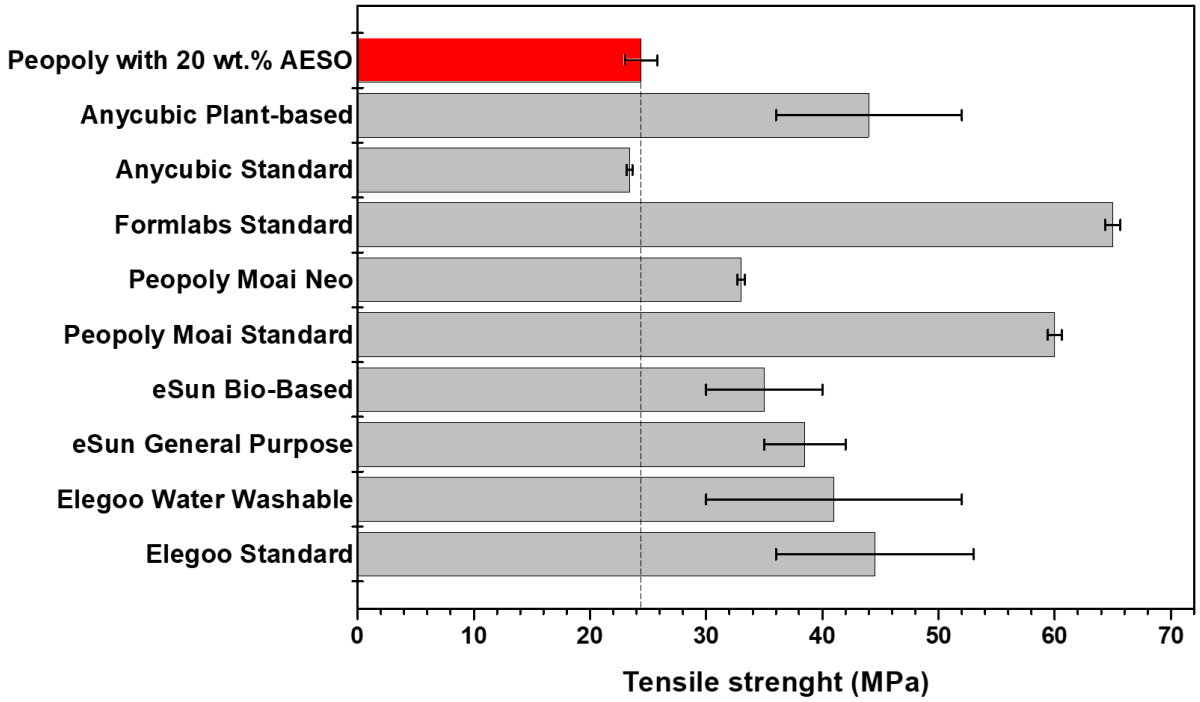


**Figure 3:** Tensile strength comparison between Peopoly moai standard with 20 wt.% EASO and different types of commercial resins.

The elongation at break is directly related to the material ductility. High ductility allows the structures to bend and deform to some extent without cracking.[41] The elongation at the break of the mixture increased as the EASO content increased, as shown in Figure 4. The maximum elongation at break of pure Peopoly resin is 2.3%. It increased to 2.9 and 4.8% (108% higher than pure PY) when the EASO content was 10 and 50 wt.%, respectively. Cui et al. [17] observed similar behavior when 20 wt.% of urethane epoxidized soybean oil was incorporated into the resin system, which increased the elongation by approximately 13%.[17] The improvement of the samples flexibility and elongation at break with the addition of EASO is in accordance with the

findings by Zhang et al.[42], where it was assigned to the presence of free fatty acid chains from the soybean oil, which act as plasticizers.[42]

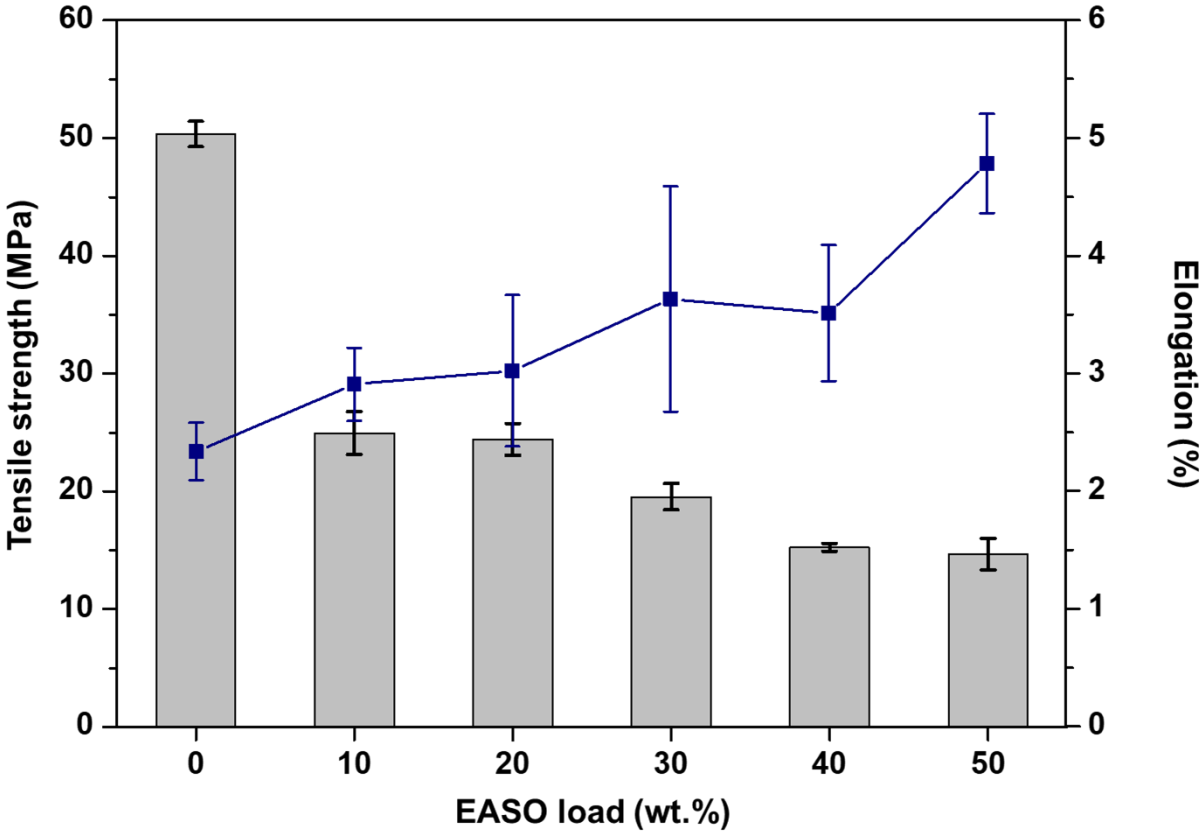


**Figure 4:** Variation of the tensile strength (gray bars) and elongation (blue squares) as a function of EASO loadings. Statistical analysis for the elongation at break was done using a one-way analysis of variance (ANOVA) with the level of significance set at probabilities of $p < 0.05$.

The fracture energy, which is the area under a stress-strain curve, is known to have a direct relationship with the material toughness. In materials with high crosslinking density, toughness tends to decrease.[43] PY toughness decreased by 19.4% with the incorporation of 10 wt.% of EASO (Figure 5a); further increasing the EASO content did not affect this parameter. Besides, Young modulus, as shown in Figure 5b, is negatively impacted by the incorporation

of EASO dropping down from 2.15 to 0.55 GPa (74.4% decrease) when 50 wt.% of EASO was incorporated. Similar to the tensile strength, the reason for the decrease is attributable to the network loosening of the polymer structure.

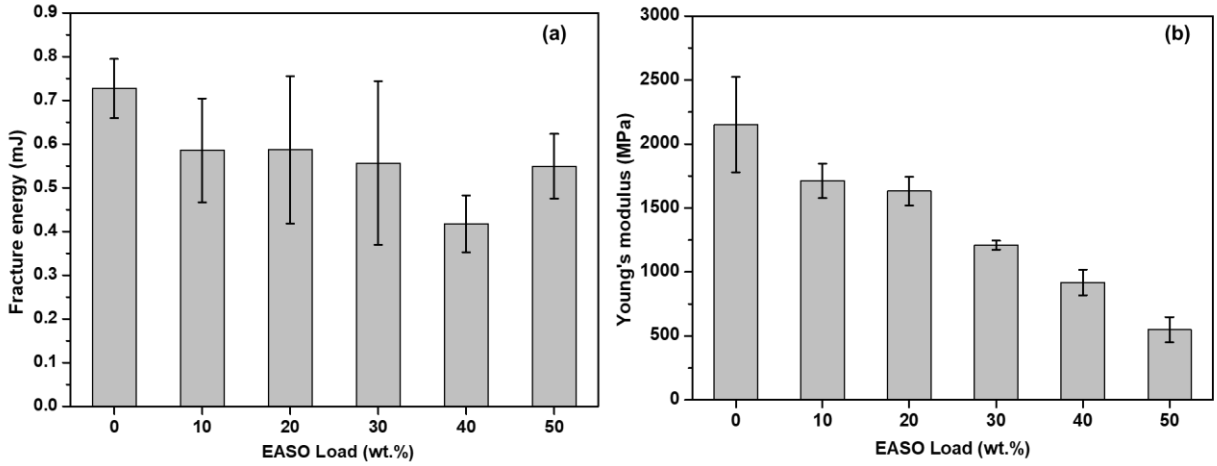


**Figure 5:** (a) Fracture energy (b) Young's modulus for 3D-printed samples with varying EASO loadings.

### 3.4 Thermogravimetric analyses

Thermogravimetric analyses were performed in order to assess the thermal and thermo-oxidative stability of the different UV-cured systems. Table 1 collects the obtained data.

Table 1: thermogravimetric data for the different UV-cured systems

| Sample code | Atmosphere | $T_{5\%}$ [ºC] | $T_{max1}$[a] [°C] | Residue at $T_{max1}$ [%] | $T_{max2}$[a] [°C] | Residue at $T_{max2}$ [%] | Residue at 700 °C [%] |
|---|---|---|---|---|---|---|---|
| PY | nitroge | 316 | 429 | 41 | - | - | 5.1 |
| $PYEASO_{10}$ | | 318 | 432 | 39 | - | - | 4.7 |
| $PYEASO_{20}$ | | 300 | 433 | 37 | - | - | 3.8 |

| | | | | | | | |
|---|---|---|---|---|---|---|---|
| $PYEASO_{30}$ | | 308 | 429 | 40 | - | - | 3.3 |
| $PYEASO_{40}$ | | 311 | 432 | 38 | - | - | 3.0 |
| $PYEASO_{50}$ | | 280 | 426 | 40 | - | - | 1.3 |
| EASO | | 308 | 390 | 59 | - | - | 2.7 |
| PY | | 311 | 421 | 51 | 555 | 8.8 | 0 |
| $PYEASO_{10}$ | | 320 | 428 | 45 | 554 | 8.1 | 0 |
| $PYEASO_{20}$ | | 305 | 428 | 47 | 551 | 7.8 | 0 |
| $PYEASO_{30}$ | | 307 | 427 | 48 | 543 | 7.4 | 0 |
| $PYEASO_{40}$ | air | 303 | 425 | 49 | 555 | 7.2 | 0 |
| $PYEASO_{50}$ | | 291 | 423 | 49 | 551 | 6.8 | 0 |
| EASO | | 293 | 397 | 54 | 552 | 5.7 | 0 |

[a] From derivative curves.

The obtained data seem to indicate a very limited effect provided by the introduction of increasing amounts of the bio-based resin in PY: in fact, regardless of the composition of the UV-cured products, the changes of $T_{5\%}$, $T_{max1}$ and $T_{max2}$ values are very limited. Besides, it is worth noticing a slightly higher charring effect provided by PY with respect to EASO, with a monotonic decrease of the residues in nitrogen at the end of the TGA tests, increasing the EASO content.

### 3.5 Effect of EASO on PY wettability

Hydrophilicity is known to be directly correlated with the ability to promote cell adhesion and proliferation, which are important factors for biocompatible materials.[19,44] In order to verify the influence of EASO addition on the wettability of printed samples, static contact angle (CA) measurements were performed. As shown in Figure 7, neat PY and EASO

printed resins have a contact angle of 72.2º and 30.8º, respectively. Despite EASO contains hydrophobic long-chain non-polar fatty acid chains that could increase the hydrophobicity of samples, the static contact angle value is lower as compared to the Peopoly-printed sample. This can be explained by the low number of polar groups in cured Peopoly resin, which limits its wettability. As expected, the incorporation of EASO into Peopoly significantly reduced CA values of the commercial resin, reaching 53.6º when 50 wt.% of EASO was added.

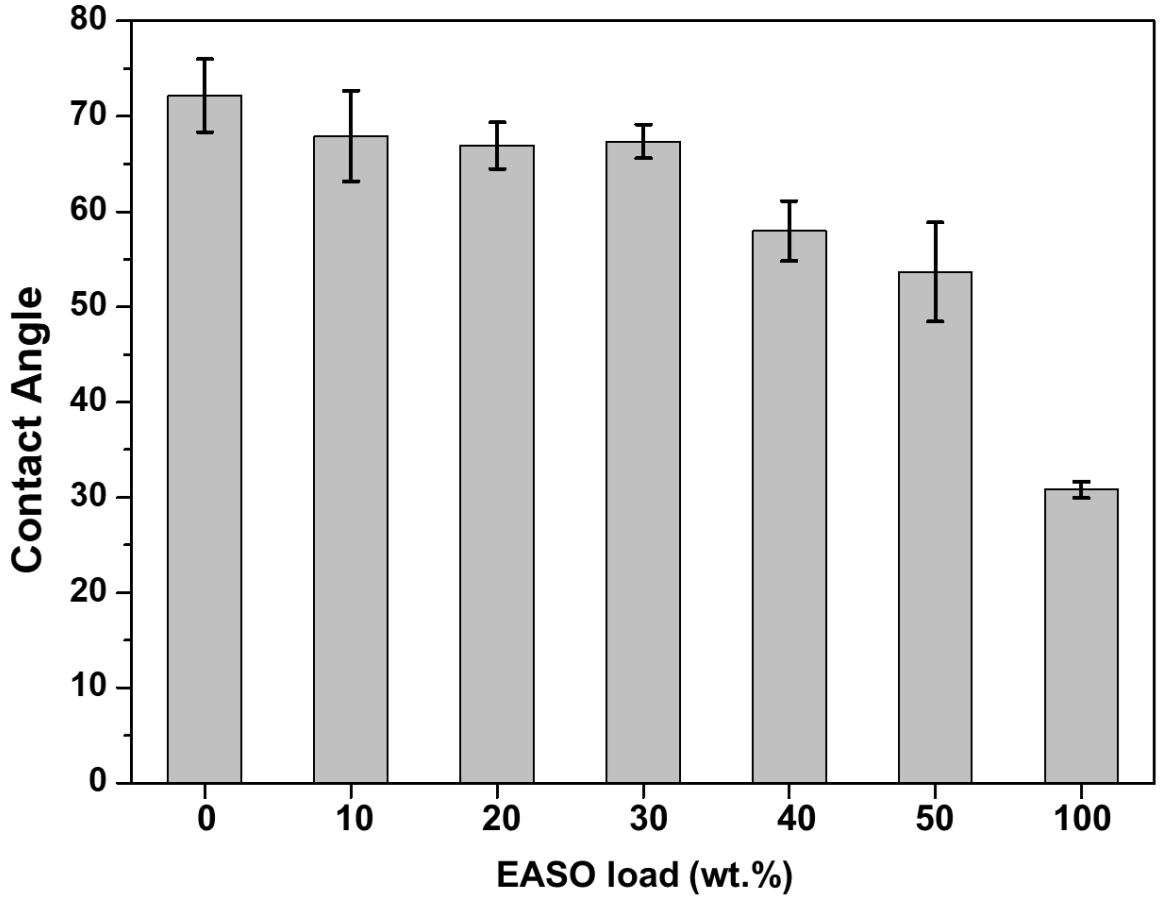


**Figure 6:** Water contact angle measurements of 3D-printed samples with different EASO loadings. Statistical analysis for the contact angle was carried out using a one-way analysis of variance (ANOVA) with the level of significance set at probabilities of $p < 0.05$.

### 3.6 Swelling properties

Swelling is defined as an increment in the volume of a solid or gel when in contact with a gas or liquid. [46] The change in volume can lead to various deformation on the swollen material,

such as wrinkles and surface breaks, which is crucial to avoid when designing implants and prothesis [19,47] or when structural applications are considered.[48]

Two factors are known to influence the swelling properties of polymers, the crosslinking density and hydrophilicity.[49] Polymers with high crosslinking density have shown to absorb less water, due to a highly entangled chain structure, which prevents water to enter.[50] On the other hand, material with high hydrophilicity are known to absorb water more easily.[49] The EASO and PY mixture is a good example of how these two properties can influence the swelling behavior of the parts.

As shown in Figure 7, the addition of EASO in the PY resin promoted an overall increase of the wettability of obtained PY/EASO UV-cured mixtures. The incorporation of 10 wt.% of EASO into the PY resin increased the swelling from 0.13% to 1.4% and 2.2% after 5 and 30 days, respectively. When 50 wt.% of EASO was added, the swelling increased only by 1.0 and 1.2%, respectively, during the same period of time. However, all PY/EASO mixtures showed higher swelling than their pure counterparts. The higher swelling of the PY/EASO mixtures could be due to opposite swelling characteristics of pure EASO and PY.

As shown by the contact angle analysis (Figure 6), PY is hydrophobic, while EASO is hydrophilic. Even though EASO has long carboxylic chains (hydrophobic), according to Liu et al.[51] EASO contains polar groups in its structure (hydroxy and epoxy groups), which are responsible for the inherent water absorption capability.[51] Thus, by adding EASO, the swelling of the mixture increases, but at the same time the crosslinking density increases, which decreases the swelling. This balance could be the reason, for which the PY/EASO mixtures showed high swelling compared with their pure counterparts.

Figure 7 also demonstrates that all PY/EASO UV-cured mixtures showed swelling stability after 20 days in water; besides, pure UV-cured PY and EASO had the higher swelling rates (about 686% and 81%, respectively, during the 30 days period). ~~All the~~ Finally, all the

tested samples showed mechanical integrity during 21 days of immersion in water. However, after 30 days, the mixtures containing 40 and 50 wt.% of EASO started to degrade inside the water. The degradation is attributed to the natural biodegradability of EASO and is in agreement to the results reported by Yu et al. [22]

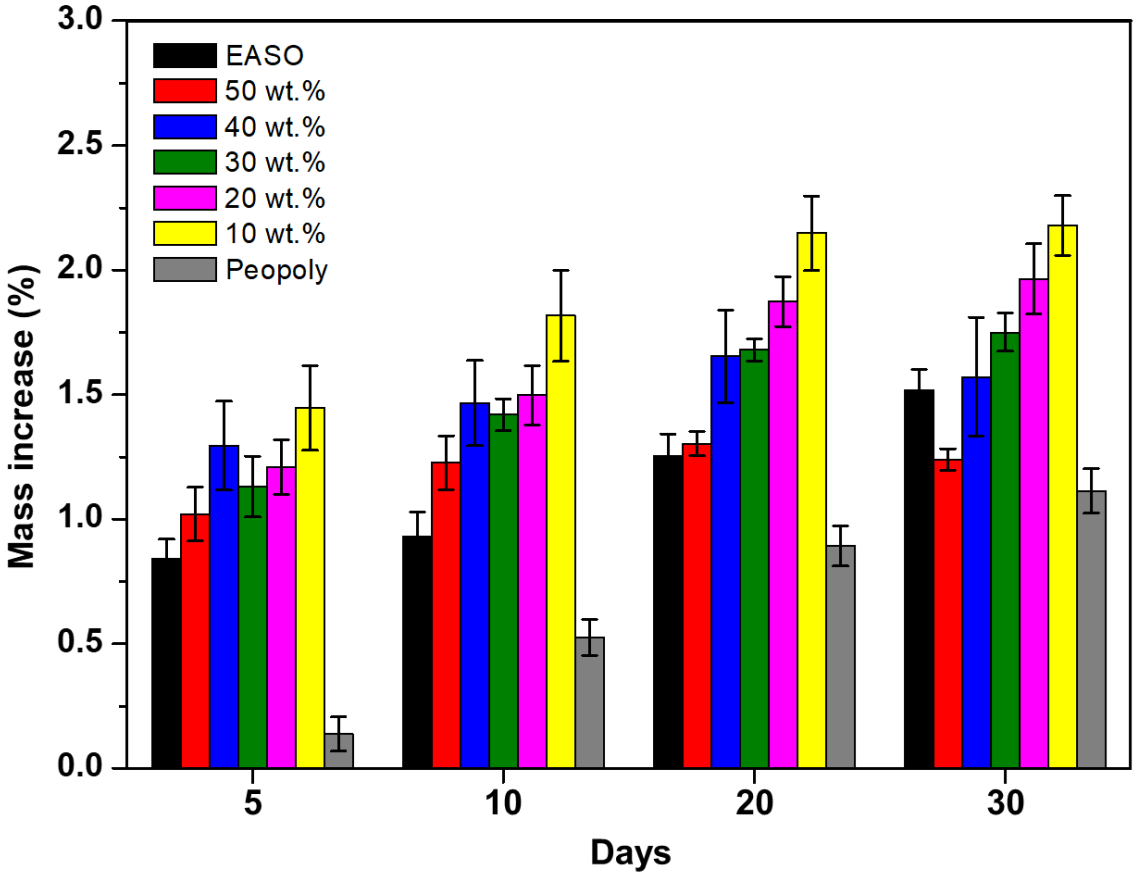


**Figure 7:** Swelling behavior of 3D-printed parts with different EASO loadings, after 5, 10, 20 and 30 days of immersion in water

### 3.7 Visual evaluation

Visual tests were carried out to compare the printing quality of mixtures containing EASO with Peopoly standard. The liquid resin did not show phase separation (or sedimentation) phenomena before being used to print the prototypes. As shown in Figure 8, three boat prototypes (3DBenchy) were printed with 0, 10, and 50 wt.% of EASO (samples A, B and C of Figure 8, respectively). The yellowish color observed for samples B and C is derived from the

EASO, which naturally has a yellow color, as reported by Miao et al.[23] and Kasetaite et al.[52] and it is not related to the post curing process.[23,52]Moreover, close visual inspection of the printed samples (Figures 8A*, 8B* and 8C*) demonstrated good printing quality and smooth surfaces, which are worthy indications for commercial suitability.

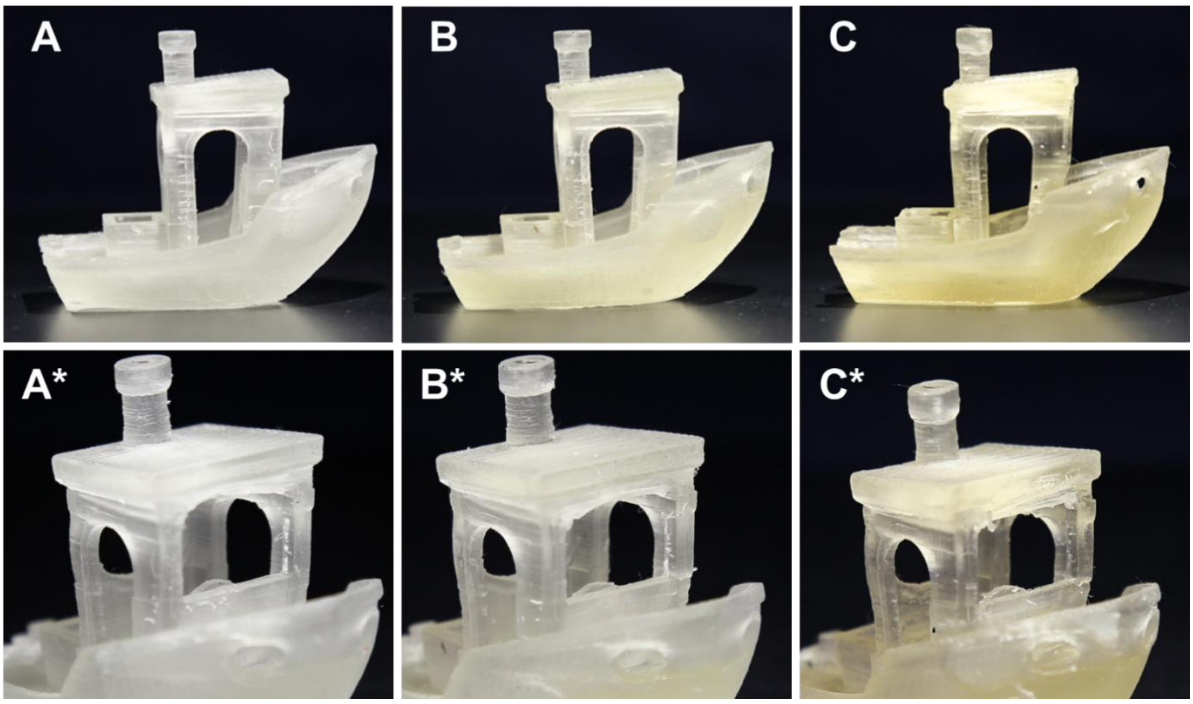


**Figure 8:** Digital images of the boat prototypes (48 x 24.8 x 38.4 mm) printed with different EASO concentrations. Boat A was printed with pure Peopoly resin and boats B and C with 10 and 50 wt.% of EASO mixed in it. The images A*, B* and C* are close-ups of their respective counterparts.

## 4 CONCLUSIONS

This study demonstrated the feasibility of combining epoxy-acrylate soybean oil with a standard resin used for 3D printing applications. The EASO content ranged from 10 to 50 wt.%, and the FT-IR investigation demonstrated that the photoinitiator present in the resin was enough to drive the UV-curing process. Besides, as assessed by rheological analyses, the presence of up to 50 wt.% of EASO in the formulations allowed maintaining the viscosities in a range

suitable for SLA 3D printing. The addition of 50 wt.% of EASO into the PY resin resulted in a decrease in both tensile strength and Young's modulus by 70.9 and 74.4%, respectively, due to network loosening. Nevertheless, the tensile strength loss was compensated with an improvement of the elongation at break: this latter was increased by 108% when 50 wt.% EASO was added to PY. Additionally, the mixtures containing 10, 20 and 30 wt.% of EASO showed mechanical properties similar to other commercial resins (with clear improvements in flexibility).

Visual assessment of the samples highlighted that the PY-EASO formulations were suitable for 3D printing complex structures, hence indicating that the epoxy-acrylate soybean oil could partially replace petroleum-based resins without affecting the printability. The incorporation of EASO into the Peopoly resin did not show any remarkable effect on either the thermal or thermo-oxidative stability of the UV-cured products. Among all the investigated formulations, 30 wt.% EASO loading was found to be the most promising, as it exhibited mechanical properties similar to fossil-based commercial resins. Further analyses and experiments have to be performed to increase the "bio" content in the fossil-based formulation, to optimize the mechanical properties, as well as to deeply study the resin biodegradability and biocompatibility. However, the proposed approach seems to be an effective starting point toward the development of environmentally friendly materials.

## DECLARATION OF CONFLICTING INTERESTS

The author(s) declared no potential conflicts of interest with respect to the research, authorship, and/or publication of this article.

## ACKNOWLEDGEMENTS

The authors would like to thank Professor Sergio Lorenzi (Department of Engineering and Applied Science - University of Bergamo) for his help in the mechanical test of samples.

**REFERENCES AND NOTES**


1. Mitchell, A.; Lafont, U.; Hołyńska, M.; Semprimoschnig, C. *Addit. Manuf.* **2018**, *24*, 606.
2. Ngo, T. D.; Kashani, A.; Imbalzano, G.; Nguyen, K. T. Q.; Hui, D. *Compos. Part B Eng.* **2018**, *143*, 172.
3. Gibson, I.; Rosen, D. W.; Stucker, B. *Addit. Manuf. Technol. Rapid Prototyp. to Direct Digit. Manuf.* **2010**, 1.
4. Tofail, S. A. M.; Koumoulos, E. P.; Bandyopadhyay, A.; Bose, S.; Donoghue, L. O.; Charitidis, C. *Mater. Today* **2018**, *21*, 22.
5. Jacobs, P. F.; Reid, D. T.; Computer; of SME., A. S. A. *Rapid Prototyping & Manufacturing: Fundamentals of Stereolithography*; Society of Manufacturing Engineers, **1992**.
6. ISO/ASTM 52900 Additive manufacturing - General principles - Terminology **2018**.
7. Vyavahare, S.; Teraiya, S.; Panghal, D.; Kumar, S. *Rapid Prototyp. J.* **2020**, *26*, 176.
8. Singh, R.; Garg, H. K. *Fused Deposition Modeling – A State of Art Review and Future Applications*; Elsevier Ltd., **2016**.
9. Ziaee, M.; Crane, N. B. *Addit. Manuf.* **2019**, *28*, 781.
10. Bagheri, A.; Jin, J. *ACS Appl. Polym. Mater.* **2019**, *1*, 593.
11. Dizon, J. R. C.; Espera, A. H.; Chen, Q.; Advincula, R. C. *Addit. Manuf.* **2018**, *20*, 44.
12. Grand View Research *3D Printing Market Size, Share & Trends Analysis Report By Material, By Component (Hardware, Services), By Printer Type (Desktop, Industrial), By Technology, By Software, By Application, By Vertical, And Segment Forecasts, 2020 - 2027*; **2020**.
13. Skoog, S. A.; Goering, P. L.; Narayan, R. J. *J. Mater. Sci. Mater. Med.* **2014**, *25*, 845.
14. Quan, H.; Zhang, T.; Xu, H.; Luo, S.; Nie, J.; Zhu, X. *Bioact. Mater.* **2020**, *5*, 110.

15. Barone, S.; Neri, P.; Paoli, A.; Razionale, A. V.; Tamburrino, F. *Procedia Manuf.* **2019**, *38*, 1017.

16. Dijkstra, P.; Tietema, M.; Folkersma, R.; Voet, V. S. D.; Strating, T.; Loos, K.; Woortman, A. J. J.; Schnelting, G. H. M.; Jager, J.; Xu, J. *ACS Omega* **2018**, *3*, 1403.

17. Cui, Y.; Yang, J.; Lei, D.; Su, J. *Ind. Eng. Chem. Res.* **2020**, *59*, 11381.

18. Lebreton, L.; Andrady, A. *Palgrave Commun.* **2019**, *5*, 6.

19. Palaganas, N. B.; Mangadlao, J. D.; De Leon, A. C. C.; Palaganas, J. O.; Pangilinan, K. D.; Lee, Y. J.; Advincula, R. C. *ACS Appl. Mater. Interfaces* **2017**, *9*, 34314.

20. Bassett, A. W.; Honnig, A. E.; Breyta, C. M.; Dunn, I. C.; La Scala, J. J.; Stanzione, J. F. *ACS Sustain. Chem. Eng.* **2020**, *8*, 5626.

21. Guit, J.; Tavares, M. B. L.; Hul, J.; Ye, C.; Loos, K.; Jager, J.; Folkersma, R.; Voet, V. S. D. *ACS Appl. Polym. Mater.* **2020**, *2*, 949.

22. Wu, B.; Sufi, A.; Ghosh Biswas, R.; Hisatsune, A.; Moxley-Paquette, V.; Ning, P.; Soong, R.; Dicks, A. P.; Simpson, A. J. *ACS Sustain. Chem. Eng.* **2020**, *8*, 1171.

23. Miao, S.; Zhu, W.; Castro, N. J.; Nowicki, M.; Zhou, X.; Cui, H.; Fisher, J. P.; Zhang, L. G. *Sci. Rep.* **2016**, *6*, 27226.

24. Liu, C.; Dai, Y.; Hu, Y.; Shang, Q.; Feng, G.; Zhou, J.; Zhou, Y. *ACS Sustain. Chem. Eng.* **2016**, *4*, 4208.

25. Wu, Q.; Hu, Y.; Tang, J.; Zhang, J.; Wang, C.; Shang, Q.; Feng, G.; Liu, C.; Zhou, Y.; Lei, W. *ACS Sustain. Chem. Eng.* **2018**, *6*, 8340.

26. Chiu, S.-H.; Wu, D.-C. *J. Appl. Polym. Sci.* **2008**, *107*, 3529.

27. Skliutas, E.; Lebedevaite, M.; Kasetaite, S.; Rekštytė, S.; Lileikis, S.; Ostrauskaite, J.; Malinauskas, M. *Sci. Rep.* **2020**, *10*, 9758.

28. Lebedevaite, M.; Ostrauskaite, J.; Skliutas, E.; Malinauskas, M. *J. Appl. Polym. Sci.* **2020**, *137*, 48708.

29. Zareanshahraki, F.; Mannari, V. *Int. J. Cosmet. Sci.* **2018**, *40*, 555.

30. Lebedevaite, M.; Talacka, V.; Ostrauskaite, J. *J. Appl. Polym. Sci.* **2021**, *138*, 50233.

31. Barkane, A.; Platnieks, O.; Jurinovs, M.; Gaidukovs, S. *Polym. Degrad. Stab.* **2020**, *181*, 109347.

32. Lin, Y. H.; Liao, K. H.; Chou, N. K.; Wang, S. S.; Chu, S. H.; Hsieh, K. H. *Eur. Polym. J.* **2008**, *44*, 2927.

33. Tathe, D. S.; Jagtap, R. N. *J. Coatings Technol. Res.* **2015**, *12*, 187.

34. Li, C.; Xiao, H.; Wang, X.; Zhao, T. *J. Clean. Prod.* **2018**, *180*, 272.

35. Jiao, Z.; Wang, X.; Yang, Q.; Wang, C. *Polym. Bull.* **2017**, *74*, 2497.

36. Jančovičová, V.; Mikula, M.; Havlínová, B.; Jakubíková, Z. *Prog. Org. Coatings* **2013**, *76*, 432.

37. Salih, A. M.; Ahmad, M. Bin; Ibrahim, N. A.; HjMohd Dahlan, K. Z.; Tajau, R.; Mahmood, M. H.; Yunus, W. M. Z. W. *Molecules* **2015**, *20*, 14191.

38. Weng, Z.; Zhou, Y.; Lin, W.; Senthil, T.; Wu, L. *Compos. Part A Appl. Sci. Manuf.* **2016**, *88*, 234.

39. Skliutas, E.; Kasetaite, S.; Jonušauskas, L.; Ostrauskaite, J.; Malinauskas, M. *Opt. Eng.* **2018**, *57*, 1.

40. Park, S.-J.; Jin, F.-L.; Lee, J.-R. *Mater. Sci. Eng. A* **2004**, *374*, 109.

41. Hiemenz, P.; Lodge, T. *Polymer chemistry*; **2007**.

42. Zhang, C.; Yan, M.; Cochran, E. W.; Kessler, M. R. *Mater. Today Commun.* **2015**, *5*, 18.

43. Ligon-Auer, S. C.; Schwentenwein, M.; Gorsche, C.; Stampfl, J.; Liska, R. *Polym. Chem.* **2016**, *7*, 257.

44. Hoffman, A. S. *Adv. Drug Deliv. Rev.* **2002**, *54*, 3.

45. Ge, X.; Yu, L.; Liu, Z.; Liu, H.; Chen, Y.; Chen, L. *Int. J. Biol. Macromol.* **2019**, *125*,

370.

46. IUPAC Swelling definition. *Goldbook*. https://goldbook.iupac.org/terms/view/S06202.

47. Hassan, M.; Dave, K.; Chandrawati, R.; Dehghani, F.; Gomes, V. G. *Eur. Polym. J.* **2019**, *121*, 109340.

48. Sienkiewicz, A.; Krasucka, P.; Charmas, B.; Stefaniak, W.; Goworek, J. *J. Therm. Anal. Calorim.* **2017**, *130*, 85.

49. Omer, R. A.; Hughes, A.; Hama, J. R.; Wang, W.; Tai, H. *J. Appl. Polym. Sci.* **2015**, *132*, n/a.

50. Grauzeliene, S.; Valaityte, D.; Motiekaityte, G.; Ostrauskaite, J. *Materials (Basel).* **2021**, *14*, 2675.

51. Liu, W.; Fei, M.; Ban, Y.; Jia, A.; Qiu, R. *Polymers (Basel).* **2017**, *9*, 541.

52. Kasetaite, S.; De la Flor, S.; Serra, A.; Ostrauskaite, J. *Polymers (Basel).* **2018**, *10*, 439.

## GRAPHICAL ABSTRACT